Modeling dissolved and particulate organic carbon dynamics at basin and sub-basin scales

Francesco Di Grazia [a,b], Xavier Garcia [c,d], Vicenç Acuña [c,d], Oriana Llanos-Paez [c,d], Luisa Galgani [a,b,e], Bruna Gumiero [f], Steven A. Loiselle [a,b,*]

[a] Department of Biotechnology, Chemistry and Pharmacy, DBCF, University of Siena, Via Aldo Moro 2, 53100 Siena, Italy
[b] CSGI, Center for Colloids and Surface Science, via della Lastruccia 3, 50019 Sesto Fiorentino, Italy
[c] Catalan Institute for Water Research, ICRA, Carrer Emili Grahit 101, 17003 Girona, Spain
[d] University of Girona, Plaça de Sant Domènec 3, 17004 Girona, Spain
[e] GEOMAR Helmholtz Center for Ocean Research Kiel, Düsternbrooker Weg 20, D-24105 Kiel, Germany
[f] Department of Biological, Geological and Environmental Sciences, BiGeA, University of Bologna, Via Selmi 3, 40126 Bologna, Italy

HIGHLIGHTS

- Riverine DOC and POC dynamics reflect sub-basin land use and climate conditions.
- Semi-distributed mass balance models show spatial and temporal changes.
- An open source QGIS plug-in allows for scenario analysis of alternative land uses.
- Future climate scenarios show major reductions of riverine DOC and POC export.

GRAPHICAL ABSTRACT
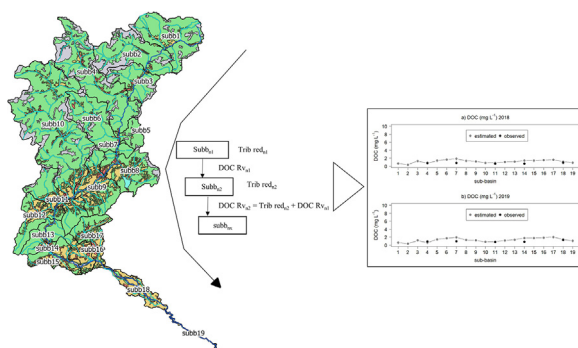
ARTICLE INFO

Editor: Ashantha Goonetilleke

ABSTRACT

Dissolved organic carbon (DOC) and particulate organic carbon (POC) play a fundamental role in biogeochemical cycles of freshwater ecosystems. However, the lack of readily available distributed models for carbon export has limited the effective management of organic carbon fluxes from soils, through river networks and to receiving marine waters. We develop a spatially semi-distributed mass balance modeling approach to estimate organic carbon flux at a sub-basin and basin scales, using commonly available data, to allow stakeholders to explore the impacts of alternative river basin management scenarios and climate change on riverine DOC and POC dynamics. Data requirements, related to hydrological, land-use, soil and precipitation characteristics are easily retrievable from international and national databases, making it appropriate for data-scarce basins. The model is built as an open-source plugin for QGIS and can be easily integrated with other basin scale decision support models on nutrient and sediment export.

We tested the model in Piave river basin, in northeast Italy. Results show that the model reproduces spatial and temporal changes in DOC and POC fluxes in relation to changes in precipitation, basin morphology and land use across different sub-basins. For example, the highest DOC export were associated with both urban and forest land use classes and during months of elevated precipitation. We used the model to evaluate alternative land use scenarios and the impact of climate on basin level carbon export to Mediterranean.

* Corresponding author at: Department of Biotechnology, Chemistry and Pharmacy, DBCF, University of Siena, Via Aldo Moro 2, 53100 Siena, Italy.
E-mail addresses: francesco.digrazia@student.unisi.it (F. Di Grazia), xgarcia@icra.cat (X. Garcia), vacuna@icra.cat (V. Acuña), ollanos@icra.cat (O. Llanos-Paez), lgalgani@geomar.de (L. Galgani), bruna.gumiero@unibo.it (B. Gumiero), loiselle@unisi.it (S.A. Loiselle).

1. Introduction

Freshwater ecosystems play an important role in regulating climate change, through their capacity to act as carbon sinks, transporters and producers (Ciais et al., 2013). Organic carbon, in both dissolved and particulate form, is a major component of the global carbon cycle and plays a fundamental role in the biogeochemical cycles of all aquatic ecosystems (Gommet et al., 2022). Both particulate (POC) and dissolved (DOC) organic carbon enter freshwater ecosystems from terrestrial ecosystems but are also produced in situ from the fixation of inorganic carbon by phytoplankton and aquatic macrophytes. The dominance of either terrestrial or internal organic carbon sources can vary depending on local conditions (Strohmeier et al., 2013). Overall, terrestrial DOC and POC loads to river networks depend both on the availability and mobility of soil organic carbon, as well as the hydrological links between land and river networks (Nakhavali et al., 2021). The concentrations of POC and DOC influence the chemical and biological dynamics of freshwater environments (Perdue et al., 1980; Roulet and Moore, 2006); as an energy source for aquatic organisms (Thurman, 1985), as an attenuator of available solar radiation (visible to UV) (Galgani et al., 2011), as well as a means of transport of macro and micronutrients and pollutants (e.g., toxic heavy metals) (Steinberg, 2003).

Biogeochemical models that consider changing hydrological conditions can provide new insights into the influence of environmental change on aquatic carbon dynamics (Aufdenkampe et al., 2011). However, few studies have used process-based models to examine the influence of land use and climate scenarios on carbon fluxes (Camino-Serrano et al., 2018). Models used to predict DOC export can range from simple regressions to complex process simulations (Supplemental Information Table 1) (Futter et al., 2007; Tian et al., 2015; Wu et al., 2014). These models differ in the definitions of the soil carbon pools, the level of detail in the process formulation (e.g., simple first-order kinetics or nonlinear relationships), and the spatial and temporal resolution. The CENTURY modeling framework (Parton et al., 1993) was one of the first models to simulate carbon sequestration services under different land-use change models. Chen et al. (2017) simulated changes in carbon sequestration under land-use change using the Dynamics of Land System (DLS) model. However, these studies did not address the links between terrestrial and instream carbon processes (Xu et al., 2019). Neff and Asner (2001) developed a DOC synthesis model, based on CENTURY, which explore DOC flux variations across a wide range of soil conditions. The sensitivity of DOC flux simulations was tested, comparing high versus low rates of DOC bioavailability and extent of DOC absorption. The Terrestrial Ecosystem Model was another process-based biogeochemical model that couples carbon, nitrogen, water, and heat processes in terrestrial ecosystems to simulate carbon and nitrogen dynamics (Melillo et al., 1993). The DocMod approach (Currie and Aber, 1997) determined DOC production in relation to forest litter decomposition, using inter-connected carbon-litter pools and related carbon transformations, with DOC production in terrestrial environment being an end-point of the overall C turn-over processes along with CO_2. Jutras et al. (2011) developed a 3-parameter DOC-3 model to extend from soil to instream DOC concentrations at a daily basin scale. Michalzik et al.' (2003) DyDOC model explored inter-connectedness of C pools and related DOC transformation, with a clear focus on forest areas. Their model driving factors were precipitation, litter production, and air or soil temperatures at hourly and daily time steps (Fröberg et al., 2007). The Acrotelm and Catotelm DOC production model considers DOC production and storage processes in peatland soil in relation to soil temperature and water-table fluctuations in the context of climate change (Worrall and Burt, 2005). The INCA-C model (Futter et al., 2007; Futter and de Wit, 2008) and the Estimating Carbon in Organic Soils Sequestration and Emissions model (Smith et al., 2010) provided estimates of instream DOC concentrations as well as production, transfer, and mineralization estimates. This model works in forested and mixed land-use basins using daily time series of soil and atmospheric conditions that can be highly variable and difficult to determinate at large basin scales. The ORCHIDEE-SOM model, within the ORCHIDEE land surface model (Krinner et al., 2005), reproduces SOC stock and DOC dynamics by simulating vertical C cycling as well as lateral exports to the river network. It provides a useful tool to explore DOC dynamics, including turnover and decomposition to CO_2, when the required data are available. The Canadian Land Surface Scheme Including Biogeochemical Cycles CLASSIC (Melton et al., 2020). CLASSIC has been used to compare the simulated mean seasonal cycle of gross primary productivity to FLUXNET observations at biome scale (Melton et al., 2020). The SWAT-C model simulates C cycle processes in terrestrial environments (Yang and Zhang, 2016; Zhang et al., 2013), and DOC cycling in river networks (Du et al., 2019), building on the approach developed previously in CENTURY. It has been used across basins of different scales and land uses (Qi et al., 2020) and most recently to model DOC dynamics at high resolution in a large and complex Canadian basin (Du et al., 2023). The SWAT model represents a major breakthrough for riverine DOC modeling, when appropriate information on soil properties (C production and mineralization), channel conditions (e.g., Manning's N) and local meteorology and hydrology are available.

Statistical modeling approaches (Ågren et al., 2010; Boyer et al., 1996; Samson et al., 2016) have also shown good results in predicting DOC production with respect to basin conditions. Lessels et al. (2015) added a DOC model to the Hydrologiska Byråns Vattenbalansavdelning (HBV) hydrological model (Lindström et al., 1997) and a DOC production module based on the static soil organic carbon (SOC) pool. A GIS based modeling framework was developed in the Regional Hydro-Ecological Simulation System (RHESSys) to simulate carbon, water, and nutrient fluxes at the watershed scale (Tague and Band, 2004), while the model by Lessels et al. (2015) also explored DOC dynamics on a basin scale. These models provide important insights to DOC fluxes, but do not address in-stream DOC processes. Moreover, their data requirements often make them less appropriate for large river basins.

In basins where data and regulatory monitoring are limited, or where stakeholders need to explore the impacts of alternative land use scenarios, the Integrated Valuation of Ecosystem Services and Trade-offs (InVEST) modeling suite (Sharp et al., 2018) has been used to estimate of carbon storage and sequestration at basin scale of major C pools (aboveground biomass, belowground biomass, soil, and dead organic matter) in relation to the spatial distribution of land use and catchment conditions. However, these models do not consider links between the terrestrial and aquatic environments and do not address instream dynamics.

There is a clear need for process-based basin-scale models of DOC and POC dynamics that consider the link between terrestrial-aquatic ecosystems as well as the instream transformations. However, for such models to be used for scenario analysis and decision support, or for basin scale analysis in regions which have limited data, a new approach is needed. This approach should be based on data that are both easily available and basin-wide, and should be complementary to other models focused on nutrient and sediment dynamics. Such a model would need to simulate fluxes considering biogeochemical transformation processes and hydrological conditions that can vary at the sub-basin scale and that would also be sensitive to climate change.

In this study, we developed an organic carbon flux model to explore the implications of river basin management scenarios at sub-basin scale on DOC and POC dynamics. The model was built to be applied as an open-source plugin for QGIS and can be used in basins with limited local data, taking advantage of international datasets and commonly available national data, for example land use and land cover, precipitation, hydrological soil properties, and topography (DEM).

2. Materials and methods

2.1. Study site

The Piave river, in the north-east of Italy, flows for 220 km into the Adriatic Sea with a drainage basin of 4500 km². Approximately 300,000 people live within the basin boundaries that fall across multiple regions (Veneto, Friuli-Venezia Giulia and Trentino-Alto Adige). The climate is temperate-humid with an average annual precipitation of ~1300 mm but

with significant spatial variations from the alpine to valley sub-basins. Land use (Fig. 1) in the upper basin (from 500 to 1800 m a.s.l.) is characterised by evergreen and deciduous forests (mainly conifers and broad-leaved trees), and alpine pasture/prairies and rock emergence present at higher elevations (above 1800 m a.s.l.). Agriculture and increased urban land classes dominate the lower part of the basin (below 500 m a.s.l.), with an increase in impervious surface cover, largely due to urban areas. Like most alpine rivers in Italy (Surian et al., 2009), the Piave River has undergone major modification to river channel dynamics and a rapid land-use change in the 20th century (Botter et al., 2010). Traditional agricultural activities on mountain slopes are increasingly being abandoned in favour of tourism, while wine production and agriculture have expanded at lower elevations. Weirs, dams and in-channel gravel mining have impacted hydrological flows and sediment transport (Comiti et al., 2011). Stakeholders need new tools to support basin scale decision making required to address conflicts in resource use, in particular with regard to climate considerations.

To explore future land-use scenarios, consultations with local stakeholders were used together with an analysis of temporal trends based on photometric and satellite-based images. This analysis showed a consistent and continuous increase in riparian vegetation within the Piave river corridor over the last five decades and a more recent trend in agricultural abandonment in the upper basin (Di Grazia et al., 2021). We used these trends to develop a 2050 scenario based on the reforestation of selected agricultural areas of the upper basin and considering changes in climate conditions based on a median emission scenario RCP 4.5 (Dezsi et al., 2018).

2.2. Carbon flux model

Dissolved and particulate carbon fluxes within a basin depend on the movement and transformation of organic carbon within individual sub-basins and within the main river. We used a mass balance approach within a spatially semi-distributed model to estimate DOC (and POC) fluxes from
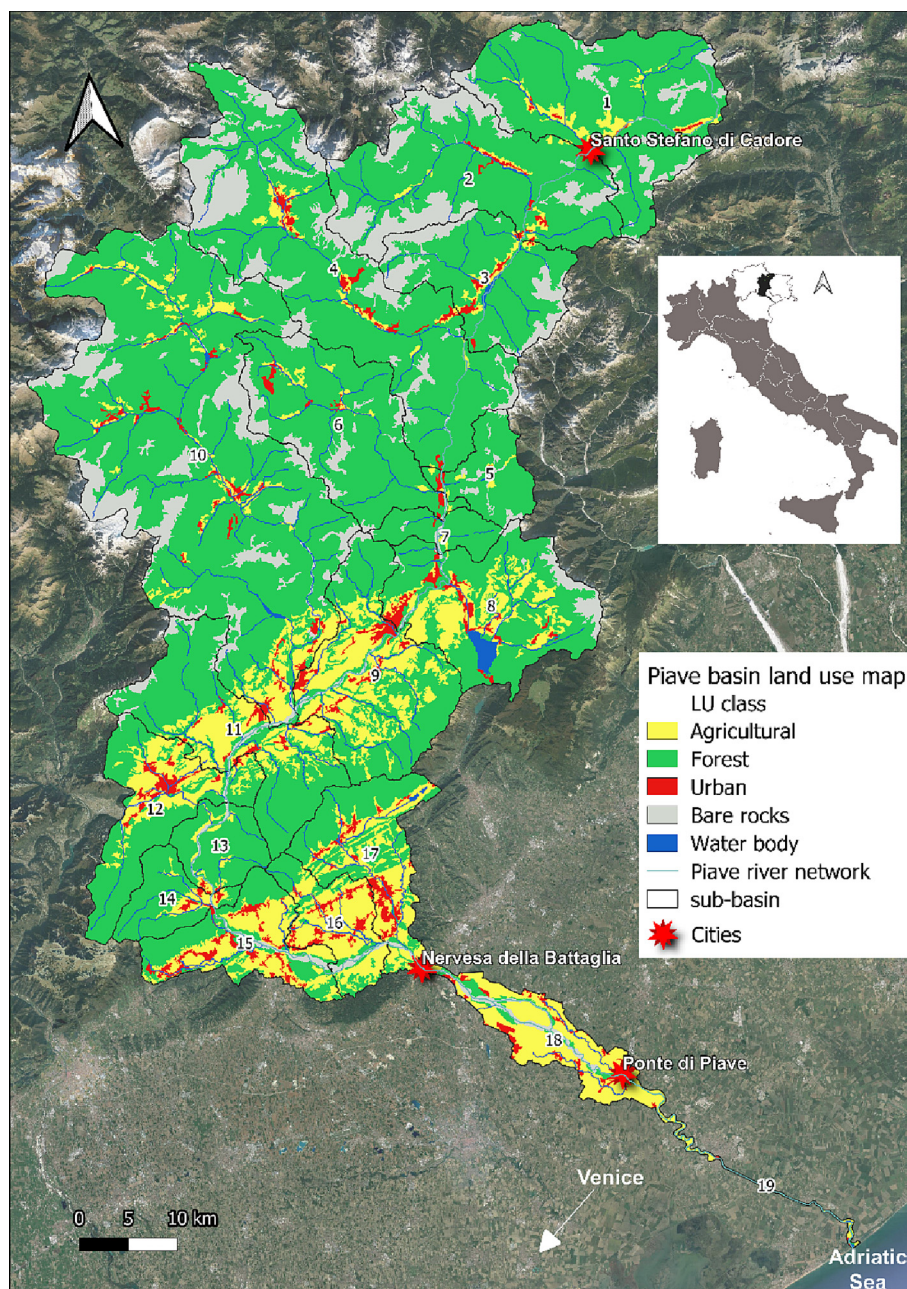

Fig. 1. Piave river basin land use (2018) based on aggregated Corine Land Use classes, showing the dominance of alpine land cover in the north and agricultural and populated areas in the middle and south. The final hydrological section of the river is heavily regulated.

the terrestrial to river environment, considering hydrological, land-use, and precipitation characteristics of individual sub-basins. More specifically, carbon flow was estimated based on DOC and POC loads of individual land uses, their transport to the river, as well as transformation processes that occur within the tributaries and the main river (per km).

Soil carbon export from each land unit (pixel) to the river were estimated based on its land use / land cover (LULC) and the distance and transport pathways to the river, based on a 20 m resolution DEM. The estimates of DOC and POC potential export for each class of LULC were obtained from concentrations reported in available scientific literature (Table 1). Where several values for a single LULC class were found, the mean value was used. Within the distributed model, these values were combined with a monthly water runoff proxy value to estimate the mass of DOC and POC reaching the tributary or river from each land use (Fig. 2).

The model simulates the movement of organic carbon (DOC, POC) within each tributary of the sub-basin and into the main river (eq. 1, Fig. 2). Within each tributary and the main river, DOC and POC loss (retention and transformation) in the sub-basin tributaries and within the main river is calculated (eq. 2). The degree of carbon reduction is also a function of the overall length of the tributaries and the main river. The governing equations are:

$$Tributary\ red_n = (DOCmass/Wn * ((100 - (tributary\ length_n * F_{D1}))/100) \quad (1)$$

$$River\ red_n = \left(\left(\left(tributary\ red_n * W_n \right) + \left(River\ red_p * \sum Wp \right) \right) / \sum W \right) \\ * ((100 - (River\ length_n * F_{D2}))/100) \quad (2)$$

$$[DOC]\ or\ (POC) = River\ red_n / \Sigma W \quad (3)$$

where the reduction factor (F_{D1} and F_{D2}, Km^{-1}) for DOC, or (F_{P1} and F_{P2}, km^{-1}) for POC, considers the reduction of organic matter in the smaller order streams and main river respectively, based on each kilometre of stream length. Tributary red and River red are the DOC and POC mass flow rates at each tributary and basin closure point (tonnes/month), river length and tributary length (km) were available from the Basin Authority. DOCmass (or POCmass) is the load (tonnes month^{-1} m^2) from each sub-basin based on land use, monthly precipitation, and soil properties. W is the water runoff proxy (m^3/month). Wp is the total flow rate from the preceding river section (m^3 month^{-1}), Wn is the total flow rate of the sub-basin section (m^3 month^{-1}).

The first sub-basin receives water from its tributaries only, without flow from any preceding river section (Wp = 0). Therefore, river DOC (or POC) is directly determined by the contribution of the tributaries present in the sub-basin and assumes no contribution from emerging groundwater (eq. 4).

$$River\ red_n = tributary\ red_n * (100 - (River\ length_n * F_{D1}))/100 \quad (4)$$

The reduction factor for DOC and POC in the tributaries in each sub-basin (F_{D1} or F_{P1}) is assumed to be constant across the sub-basin and approximates the transformation and loss of organic matter for each km of

stream length (tributary length$_n$). This reduction is applied to the transportable DOC$_{mass}$ (or POC$_{mass}$) and normalised by a runoff proxy (W) for each pixel. The result is the estimate of DOC or POC load (mg/year) transported within the sub-basin to the main river (Tributary red$_n$), occurring at the point of closure of each sub-basin. The concentration of DOC (River red$_n$) and total flow rate (W$_p$) from the preceding river section, is summed with the DOC load of the sub-basin (Tributary red$_n$ * W$_n$) to become the influx of DOC into the next sub-basin of the main river. The DOC concentration is then reduced by a riverine reduction coefficient (F$_{D2}$), considering the river length within this sub-basin, generating a DOC concentration at its closure (River red$_n$). The same approach is used for POC, where the POC river factor (F$_{P2}$) is more related to a physical retention of the POC along the river.

Longitudinal changes in DOC (or POC) concentration in the river result from LULC related sources (DOC$_{mass}$) of each sub-basin, spatial differences in precipitation, the transport and retention within sub-basin tributaries and the overall reduction within the main river section.

2.3. Organic carbon reduction factors

The composition and concentration of organic matter can be modified by photo-oxidation, microbial respiration, leaching, flocculation, sorption, and settling (Einarsdottir et al., 2017; Galy et al., 2011; Loiselle et al., 2009; Spencer et al., 2010; Von Wachenfeldt and Tranvik, 2008). Changes in longitudinal DOC and POC concentrations are determined by several factors (e.g., hydrological events, basin slope, soil C), which can have considerable spatial and seasonal variation within a basin (Li et al., 2017), with higher values in wetlands and around rainfall events (Harrison et al., 2005; Tian et al., 2015). Different models address these changes through different approaches. For example, the SWAT-C model simulates DOC and POC movement and transport through: DOC percolation coefficients; the liquid-solid partition coefficient; and POC process coefficients (Du et al., 2019; Qi et al., 2020). Camino-Serrano et al. (2018) considered that free DOC can be adsorbed to soil minerals or remain in solution based on an equilibrium distribution coefficient linked to soil properties. Gommet et al. (2022) considered differences in decomposition rates between labile and refractory DOC pools, which were geographically variable, but within the same order of magnitude. While Berggren and Al-Kharusi (2020) reported a median decomposition half-life of across multiple river sampling locations across Europe.

The initial reduction factors used in the present model were based on these past studies and then tuned by interpolation using DOC and POC measurements made in the Piave river by regional agencies in 2018 and 2019 (ARPAV, 2021a). It should be noted that there were a limited number of river sections (sub-basins) where DOC was monitored, therefore estimated reduction factors for DOC and POC loss were used to initialise the model, with final values for tributary streams, F_{D1} and F_{P1} (0.45 and 0.07 10^{-2} Km^{-1}), and for the main river sections, F_{D2} and F_{P2} (0.9 and 0.01 10^{-2} Km^{-1}) following published values. These interpolated values support earlier studies that show that deeper rivers have higher transformation and storage rates of organic matter compared to shallower and faster moving streams (Kalbitz et al., 2003). Similarly, Bouchez et al. (2014) showed

Table 1
Available studies providing information on DOC and POC concentrations in relation to different land use classes.

LU		DOC (mg L^{-1})		Data source	POC (mg L^{-1})	Data source
Forest	Broadleaved forests	17.72	20.5	(Borken et al., 2011); (Camino-Serrano et al., 2016); (Camino-Serrano et al., 2018).	0.58	(Dawson et al., 2004)
	Coniferous forests	22.55		(Borken et al., 2011); (Camino-Serrano et al., 2016); (Camino-Serrano et al., 2018).		
Agricultural	Grassland	9.17	10.18	(van den Berg et al., 2012); (Camino-Serrano et al., 2018).	1.58	(Kim et al., 2013)
	Cropland	4.2		(Camino-Serrano et al., 2018).		(Cai et al., 2015)
	Vineyard	19.2		(Cattani et al., 2006).		
Urban		24.1		(Maniquiz et al., 2010); (Ortiz-Hernández et al., 2016).	0.56	(Kalev and Toor, 2020)
Bare rocks		0			0	

DOC and POC export per sub-basin was therefore reflects the distribution of land use and the sub-basin topography, soil properties and precipitation.
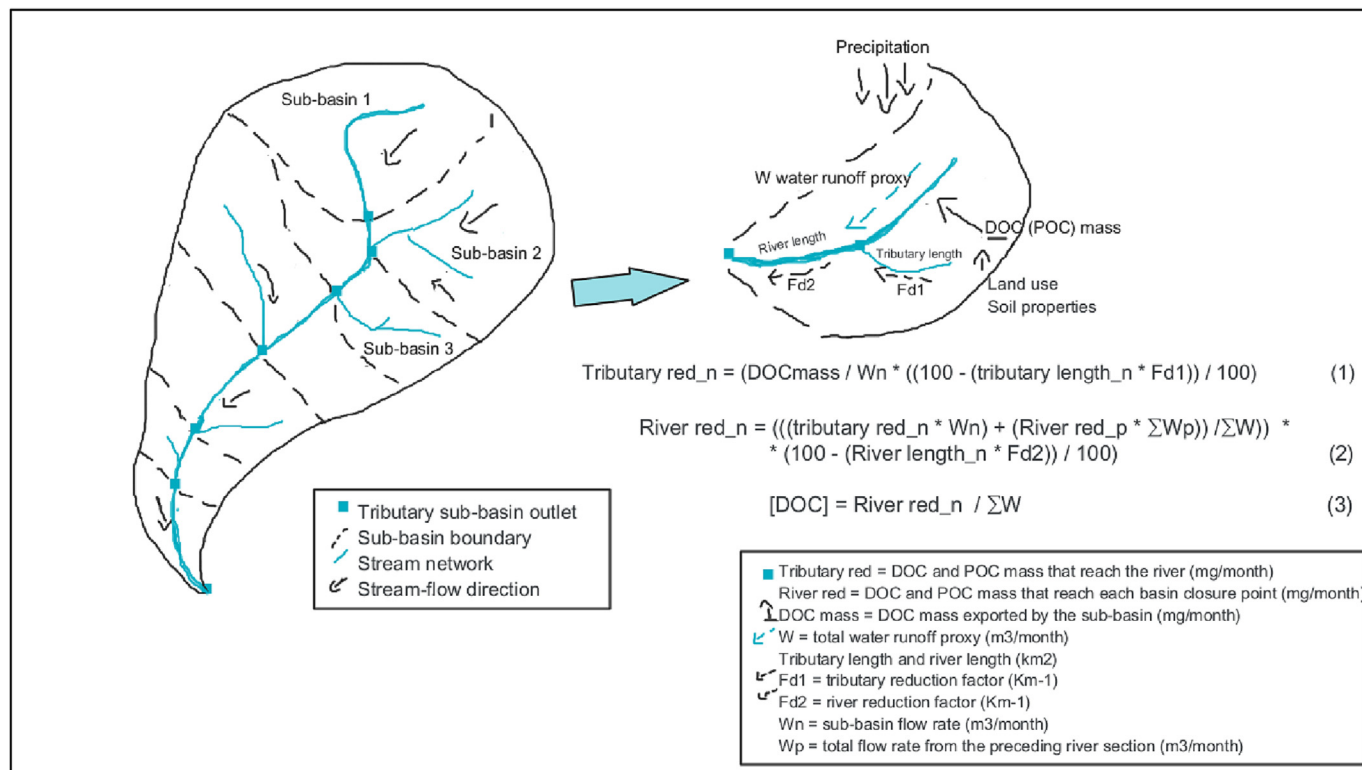
Fig. 2. DOC concentrations in the river in each sub-basin were based on the carbon transport to the river and transformation processes within the tributaries of each sub-basin (Trib red$_{n1}$, Trib red$_{n2}$) as well as those transformation processes present within the main river (DOC Rv$_{n1}$, DOC Rv$_{n2}$).

that longitudinal reductions in POC due to weathering and oxidation are more limited that those related to DOC.

2.4. Water runoff proxy

As a detailed hydrological model for the whole basin was not available, a mass balance-based approach was used to estimate the monthly surface runoff: the amount of water running off each pixel towards the river and its tributaries. It is based the Curve Number approach within the seasonal water yield model of the InVEST package (Sharp et al., 2018). The Curve Number method developed by Natural Resources Conservation Service (NRCS) of the United States Department of Agriculture (USDA) (NRCS-USDA, 2007) is widely used for predicting direct surface runoff volume for a given rainfall event and estimating the volumes and peak rates of surface runoff at basin scale (da Silva Cruz et al., 2022). A higher CN value suggests a higher runoff potential, whereas a lower CN value signifies low runoff. This approach was chosen due to its utility to explore future scenarios of land use and climate change (da Silva Cruz et al., 2022).

The model combines a digital elevation model (DEM) and commonly acquired climate and soil information from regional and international sources (Nistor et al., 2018; NRCS-USDA, 2007). It uses the basic principles of water partitioning (precipitation becoming runoff) and routing (upgradient water becoming available to downgradient parcels). These simplified routing processes allow for a large degree of uncertainty and should be interpreted as proxy of runoff rather than predictions of absolute values. The model calculates the monthly water runoff proxy of each pixel based on a modification to the NRCS curve number (NRCS-USDA, 2007), which estimates monthly direct runoff (Guswa et al., 2017; Hamel et al., 2020).

2.5. Model input data for the Piave river basin

The carbon models DOC and POC loads (mg L^{-1}) for each of five LULC classes together with the water runoff proxy (mm) and vectors files

containing the tributaries and river networks (km). Five simplified classes (artificial, agricultural, forests, bare rocks, and water bodies) were used. We identified 19 sub-basins using GRASS watershed function on QGIS Development Team (2022) while the river networks were obtained from the stream raster generated from the water runoff proxy model.

Monitored DOC concentrations were obtained from the regional environmental agency ARPAV (Agenzia Regionale per la Protezione Ambientale - Veneto) (2021a). These were very limited as DOC monitoring was initiated in 2018 and was not performed in 2021. Seasonal data from 2018 were used for model calibration. Data from 2019, from 5 stations, and from 2020 (two stations) were used for validation.

ARPAV does not monitor POC concentrations, therefore, POC was estimated by using total suspended solids (TSS) concentrations following Némery et al. (2013), eq. 5. In alpine rivers, both particulate organic carbon (POC) and particulate inorganic carbon (PIC) are closely linked to the TSS transport dynamics (Wheatcroft et al., 2010).

$$POC\% = 28.82*TSS^{-0.7499} + 0.89 \tag{5}$$

with some adjustment

$$POC = POC\%/100*TSSavg \tag{6}$$

The water runoff proxy model used a 20 m DEM available from by the national research authority (ISPRA, 2020), which was corrected to fill hydrological sinks and checked with the digital watercourse network to ensure routing along the specific tributaries using QGIS v.3.22 (2022). Basin area was obtained from the regional geoportal and based on the Water Protection Plan 2015 (ARPAV, 2021b). Monthly average precipitation raster files at 20 m resolution were interpolated using an inverse distance weighting (IDW) of information from 72 stations for 2018, 2019 and 2020 (ARPAV, 2021c). A rain events table containing the number of rain events for each month was also used. Monthly average evapotranspiration for each pixel was extrapolated from the Reference Evapotranspiration

Global Reference Evapotranspiration (Global-ET0) Version 2 dataset (Zomer and Trabucco, 2022). Land Use (LU) raster data, referred to the year 2018, was obtained from Corine Land Use Land Cover Level IV data at a 100 m resolution (ISPRA, 2018). Soil and plant evapotranspiration coefficients (Kc) were estimated for broad land use classes suggested by Allen et al. (1998). Parameters related to flow recharge and accumulation (α, β, γ) used default values ($\alpha = 1/12$, $\beta = 1$, $\gamma = 1$) based on similar rivers. Flow accumulation is calculated from the number of upstream pixels that flow into a pixel before arriving to the tributary.

2.6. Root mean square error

The comparison of estimated to measured concentrations of DOC (and POC) used the percentage root mean square error (RMSE):

$$RMSE\% = \sqrt{\frac{\sum_{i=1}^{N}(x_i - \widehat{x}_i)^2}{N}} / \overline{x}_i$$

Where x_i is the estimated values, $\widehat{x}_i$ is the observations, $\overline{x}_i$ is the average of the observed values and N the number of observations.

3. Results

3.1. Water runoff proxy

Estimated surface runoff was compared with the available data from four calibrated gauge stations from 2015 to 2020 (ARPAV, 2022). The average discharge from the lowest sub-basin for the simulated year, 2018, was 125 m^3/s. The four stations were limited to the main Piave river and most did not have a full set of monthly data, especially following the flood event of October 2018 which compromised the measurements from several stations (EFAS, 2018). The surface runoff proxy provided a similar longitudinal trend in flow rate, increasing at lower basins. Considering these five years of data, the overall accuracy was low (RMSE = 81 %), underestimating river discharge.

3.2. DOC flux

The modelled annual average DOC concentrations at 18 sub-basins closure points shows a general increase from the upper to lower basin (Table 2, Fig. 3a). It should be noted that the DOC estimates for the first sub-basin have an intrinsic uncertainty related to the lack of information on source water discharges. As the model is based on precipitation, the first sub-basin receives low DOC load from source waters, dominated by snow and groundwater.

The reduction factors (F_{D1}, F_{D2}) were refined using available DOC data (ARPAV) for 2018 from 5 stations with complete measurements. The resulting DOC estimates captured the over longitudinal trend (RMSE = 83 %, Fig. 3a).

The model, using the same reduction factors ($F_{D1} = 0.45$, $F_{D2} = 0.9$) was validated for 2019 and 2020 (RMSE = 59 %) and showed a similar trend (Fig. 3b and c). It should be noted that the contributions from two sub-basins to the DOC load of the main river were estimated to be negative (sub-basins 4 and 10), and therefore set to zero, indicating that the LULC and hydrology of these basins allowed for a net zero contribution to the DOC in the main river. These sub-basins have hydrological and land use characteristics that create conditions of limited DOC production with respect to the reduction factors for tributaries present, resulting in the equivalent of net zero DOC export.

The model was run at the monthly frequency to explore seasonal changes in DOC concentrations, along the longitudinal DOC gradient, under present land LULC and meteorological conditions of 2018 and 2019 (Supplementary Fig. 1). DOC concentrations were generally higher in June, with an average value of 1.19 mg L^{-1} (RMSE = 119 %), followed by February (1.27 mg L^{-1}, RMSE = 83 %) and December (0.86 mg L^{-1}, RMSE = 57 %). This seasonal change was most evident in the sub-basins in the middle of the basin.

3.3. POC flux

POC flux and POC concentrations showed a general increase along the longitudinal gradient, to the highest concentration at the Piave basin closure point (Table 3).

To interpolate the reduction factors ($F_{P1} = 0.07$ and $F_{P2} = 0.01$) and validate the model, we used POC estimates (eq. 5) from five sites for the years 2018 and 2019, considering the organic fraction to dominate the overall mass of TSS, based on observations for similar rivers in subalpine regions (Némery et al., 2013). The results showed that the simulated POC for the year 2018 (RMSE = 24 %) was underestimated in the two sites located in the upper basins and overestimated in the sites 11 and 14 (Fig. 4a). Particulate load in the upper basin is expected to have a higher percentage of inorganic particulates, related to snow and glacier melt and groundwater sources, typical of alpine streams (Chanudet and Filella, 2008). The underestimate in the lower river sub-basin is related to the fact that the model does not determine allochthonous production of organic particulates from primary production. The validation of the model using POC values for 2019 (Fig. 4b) and 2020 (Fig. 4c) showed a reasonable accuracy (RMSE = 41 %) with annual POC dynamics similar to 2018 (Fig. 4a). While overall longitudinal and seasonal dynamics follow expected trends, it should be noted that the direct measurement of POC, at regular intervals and for multiple years would improve both the model training as well as validation.

The model was run at the monthly frequency to compare seasonal changes in POC concentrations for present day LULC and meteorological conditions. POC concentrations were generally higher in June (Supplementary Fig. 2) with an average value of 0.43 mg L^{-1} (RMSE = 51 %), followed by February (0.33 mg L^{-1}, RMSE = 23 %) and December (0.31 mg L^{-1}, RMSE = 35 %). This was most evident in the sub-basins in the middle of the basin.

3.4. DOC & POC model plugin

The DOC & POC model plugin (Supplementary Fig. 3) was developed for open-source QGIS to allow for the analysis how modifications in land management and climate could be used to explore changes in DOC and POC export at basin and sub-basin scale. The code was written in Python using the associated QGIS Plugin Builder. QGIS is an open-source software for geographic information system (GIS) that is supported by a large community of users and developers. The DOC & POC model plugin code is downloadable from the GitHub repository (https://github.com/
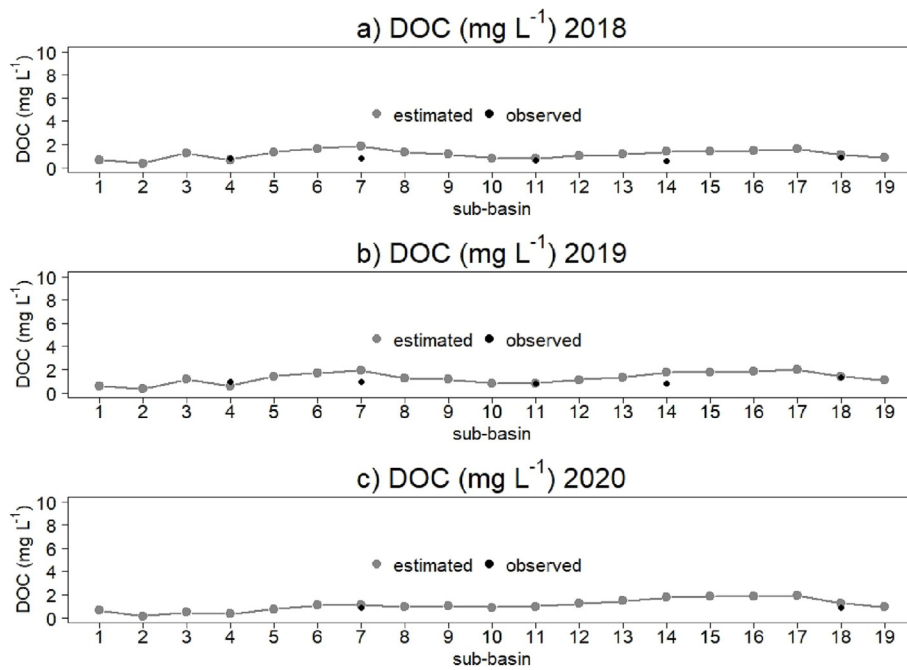
Table 2
Average annual DOC concentration and mass in each sub-basin calculated by the model following the DOC equations for the year 2018.

Sub-basin	Estimated DOC (mg L^{-1})	DOC mass (tonnes/year)
1	0.67	3.79×10^1
2	0.36	4.08×10^1
3	1.29	1.92×10^2
4	0.69	1.65×10^2
5	1.37	3.48×10^2
6	1.66	5.13×10^2
7	1.87	5.90×10^2
8	1.35	5.29×10^2
9	1.19	5.68×10^2
10	0.81	5.50×10^2
11	0.82	6.10×10^2
12	1.03	8.29×10^2
13	1.15	9.49×10^2
14	1.40	1.19×10^3
15	1.39	1.24×10^3
16	1.49	1.37×10^3
17	1.60	1.55×10^3
18	1.13	1.13×10^3
19	0.86	8.56×10^2

Fig. 3. Longitudinal distribution (logarithmic scale) of DOC concentration and comparison with the observed ARPAV values for the years 2018 (a), 2019 (b) and 2020 (c).

dgfrancesco/DOC-POC-model-Di-Grazia-et-al.-). The model plugin can be accessed from the QGIS graphical user interface by opening the Python Console and selecting 'open existing script'. The plugin is intended to be used with other GIS based scenario development tools (e.g., InVEST) that allow stakeholders to explore changes in nutrient and sediment river exports.

4. Discussion

4.1. Estimated dynamics of organic carbon export

The organic carbon (DOC and POC) dynamics across the Piave River basin showed longitudinal variations that reflected sub-basin differences in LULC, stream length, instream reduction, and surface runoff hydrology, and seasonal variations in precipitation. Seasonality in DOC and POC fluxes represents one of the major uncertainties in modeling riverine organic

Table 3
POC concentration and mass in each sub-basin calculated by the model following the POC equations for the year 2018.

Sub-basin	Estimated POC (mg L^{-1})	POC mass (tonnes/year)
1	0.37	2.10×10
2	0.33	3.75×10
3	0.33	4.96×10
4	0.32	7.61×10
5	0.33	8.38×10
6	0.34	1.04×10^2
7	0.34	1.07×10^2
8	0.40	1.57×10^2
9	0.46	2.21×10^2
10	0.40	2.47×10^2
11	0.42	3.14×10^2
12	0.44	3.58×10^2
13	0.45	3.70×10^2
14	0.45	3.83×10^2
15	0.47	4.15×10^2
16	0.48	4.46×10^2
17	0.50	4.86×10^2
18	0.51	5.07×10^2
19	0.51	5.07×10^2

matter dynamics (Gommet et al., 2022; Tian et al., 2015). In the coupled hydrology–biogeochemistry DOC model developed by Lessels et al. (2015), in-stream DOC concentrations typically followed streamflow patterns, increasing in the spring from precipitation induced DOC transport from the soil. Our model shows similar dynamics, higher DOC concentration in June linked to higher monthly rainfall (108 mm) and lower in January and December where precipitation was lower (77 and 12 mm). It should be noted that flood events are often responsible for a large part of POC and DOC transport (Bastias et al., 2020; Battin et al., 2008; Raymond et al., 2016).

Differences in sub-basin DOC and POC estimated exports show spatial variations in precipitation, basin morphology and land use, as well as soil carbon content across different alpine, subalpine and valley sub-basins. These spatial differences in expected soil erosion and mobilization of dissolved and particulate matter are supported by past studies showing the impact of these factors on river organic matter exports (Li et al., 2017; Zhang et al., 2022). The highest DOC mass concentrations were related to sub-basins dominated by urban and forest land use. The geographical distribution of DOC sources (Fig. 5a) showed the highest density in the upper and middle basin with peaks corresponding to the urban area in the middle sub-basins (sub-basins 5–12). Urban DOC export depends on multiple sources; wastewater treatment systems, road runoff, biomass burning aerosols, coal combustion, industrial activities, etc., (Aitkenhead-Peterson et al., 2009; Siudek et al., 2015). The highest POC mass concentrations were related to sub-basins dominated by agricultural land use (sub-basins 8–17) (Fig. 5b), similar to past studies showing high POC loads in agricultural areas (Luo et al., 2022).

Final DOC export to the Adriatic Sea. (sub-basin 18) showed values consistent to those measured by the regional agency, with DOC and POC exporting 856 tons/year and 506 tons/year. Changes in OC export have implications on the productivity of the Adriatic Sea, which is a narrow and shallow area of the Mediterranean Sea, where dilution is limited (Ciglenečki et al., 2020). In relation to the Po River, these fluxes are approximately 1 % of the total DOC and POC emitted (Pettine et al., 1998).

4.2. Future scenarios

The model was used to explore different scenarios of land use and climate for the Piave river basin, looking towards 2050. Based on
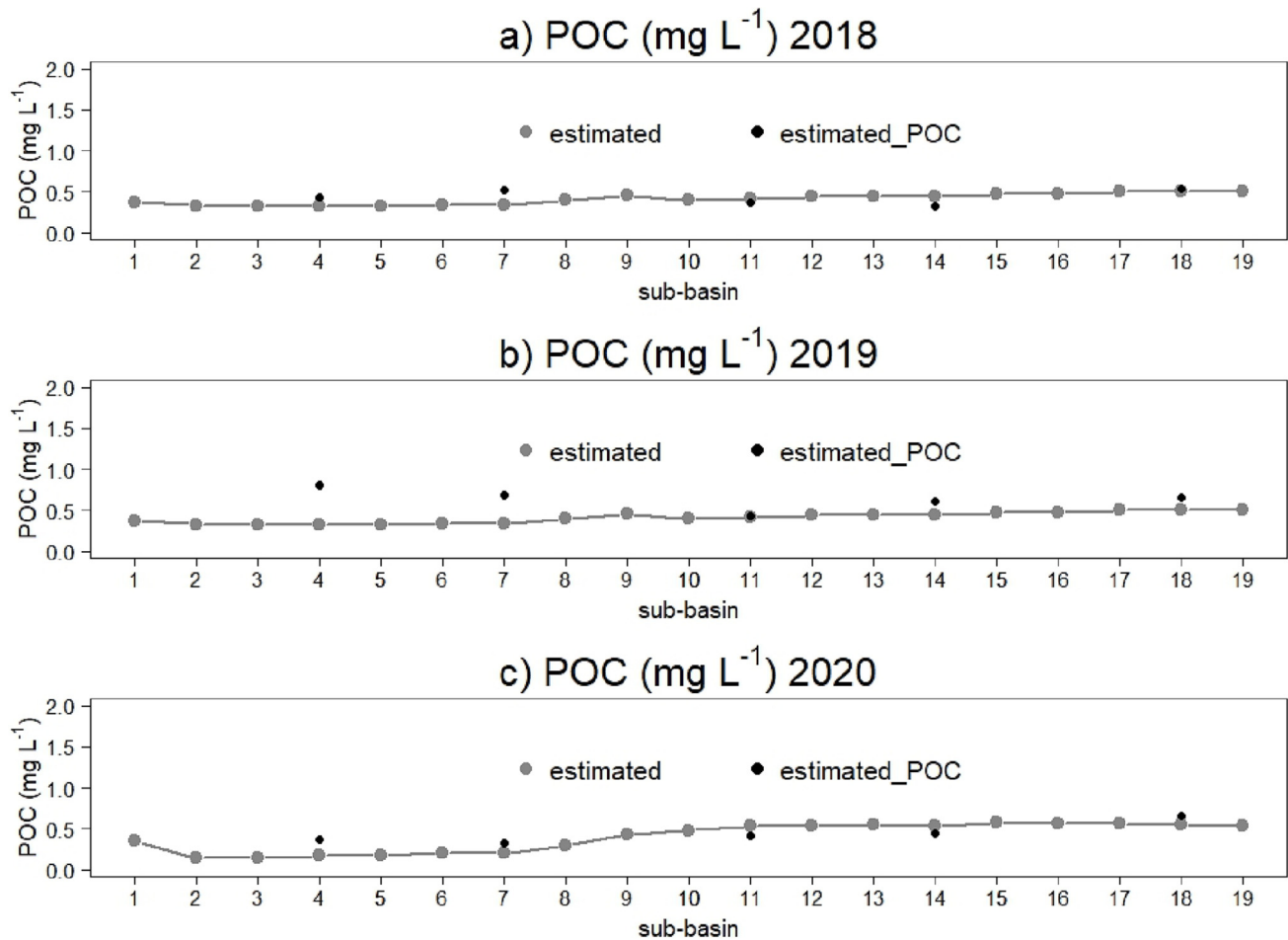
a) POC (mg L^{-1}) 2018

b) POC (mg L^{-1}) 2019

c) POC (mg L^{-1}) 2020

Fig. 4. Longitudinal distribution of POC concentration and comparison with the observed ARPAV values for the years 2018 (a), 2019 (b) and 2020 (c).

consultations with local stakeholders and a study of 50-year trends, a reforestation scenario was evaluated as the most feasible.

Looking first at projected changes in climate and based on the emission scenario RCP 4.5, a decrease in annual precipitation for the Piave Basin is expected to occur by 2050 (Dezsi et al., 2018). This will lead to a reduction in the water runoff proxy throughout the basin, due to greater evaporation and an increased hydrological deficit. This 2050 climate scenario showed a decrease in DOC export by 25 % (214 tons/year) and in POC export by 26 % (127 tons/year) with respect to 2018 export. Given an increase in the temperature and reduced runoff, it is likely that soil conditions, as well as river and tributary reduction factors will also change (increased reduction). Qu and Kroeze (2010) using the Global NEWS models estimated that, that in 2050, riverine DOC export will exceed POC in total C export. In particular, POC is expected to decrease by 15–25 % as a consequence of human perturbation, land use change and dam construction.

Looking at the combined scenario of modified land use (reforestation) and climate change (RCP 4.5), the model showed an expected reduction in DOC export by 22 % (170 tons/year) and in POC export by 30 % (153 tons/year). This is based on present day DOC and POC reduction factors.

This reduced carbon export, in combination to the expected decrease in both phosphorus and nitrogen exports for the same climate and land use scenario (Di Grazia et al., 2021) suggest a reduced eutrophication threat for the Adriatic Sea in 2050. The area of the Mediterranean Sea has a long history of eutrophication related impacts on biodiversity and ecosystem services. The expected trend in eutrophication is supported by recent studies (Ciglenečki et al., 2020) showing similar reductions in carbon and nutrient concentrations.

5. Conclusions

The spatially distributed carbon flux model developed in the present study is intended to support decision making by basin scale and sub-basin scale stakeholders, in particular with respect to scenarios of land use and climate. The model can be used, together with other scenario tools to prioritise policy and management options to reduce impacts on receiving waters and improve ecosystem services. The model was applied to a single river basin but is flexible enough basins in different climate and hydrological conditions, given the availability of information on LULC, climate, hydrology, and related indices.

Data requirements for the model are relatively limited. Most of these data can be retrieved from international and national geographic databases, making this approach available for exploring DOC and POC export in data-scarce basins. The model is refined using local data, in particular monthly or seasonal concentrations of DOC and POC at the sub-basin level. The greater number of sub-basins monitored, the more robust will be the reduction factor interpolation.

Further developments in the modeling of in-stream OC dynamics should address the different loss dynamics of labile DOC and refractory DOC fractions, as their relative decay rates are significantly different (Du et al., 2020). For example, the turnover time of labile soil OC is typically 1 to 5 years, while the turnover time of refractory fractions could reach 200–1500 years (Iravani et al., 2019). Estimates of relative percentages of labile and refractory OC, related to different LULC classes could be used to improve the model as well as include new information on estimates of CO_2 evasion from the river.
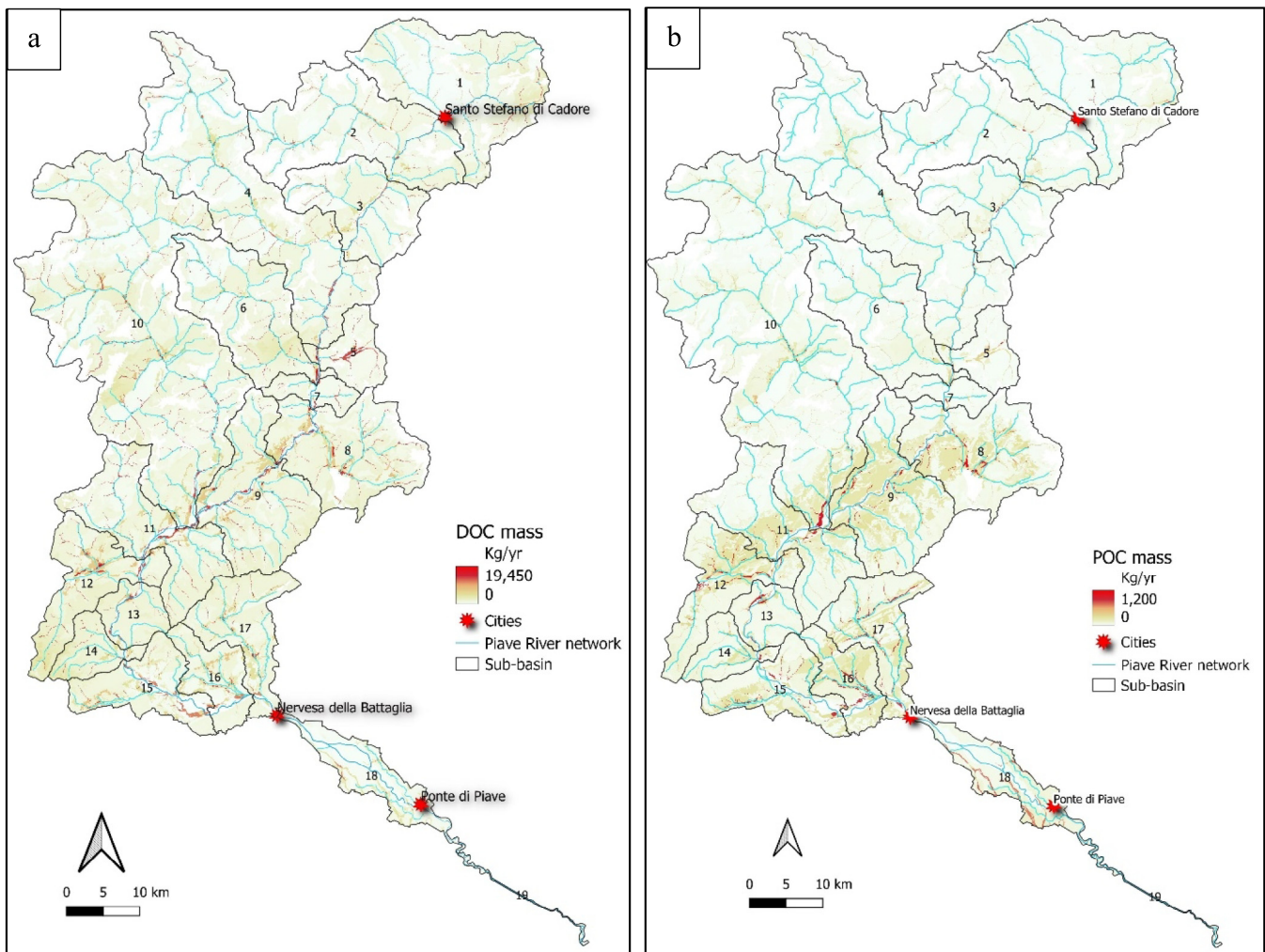
Fig. 5. Spatial distribution of DOC (a) and POC (b) across the 19 sub-basins.

The DOC and POC model was designed as a QGIS plugin for basin scale studies. The model output can be used to evaluate carbon export based on varying land use and climate scenarios, providing an additional tool to support basin management.

Supplementary data to this article can be found online at https://doi.org/10.1016/j.scitotenv.2023.163840.

CRediT authorship contribution statement

Conceptualization: F.D.G., X.G., V.A., O.L.P. and S.L.; Methodology: F.D.G, X.G., V.A., O.L.P and S.L.; Software: F.D.G. and X.G. Validation: F.D.G. and S.L.; Data curation: F.D.G., L.G., B.G. and O. L.P.; Writing - original draft: F.D.G. and S.L.; Writing - review & editing: F.D.G, L.G., B.G., O.L.P., V.A., X.G and S.L.

Data availability

The link to the DOC & POC model code repository is available on the manuscript attached file

Declaration of competing interest

The authors declare that they have no known competing financial interests or personal relationships that could have appeared to influence the work reported in this paper.

References

Ågren, A., Buffam, I., Bishop, K., Laudon, H., 2010. Modeling stream dissolved organic carbon concentrations during spring flood in the boreal forest: a simple empirical approach for regional predictions. J. Geophys. Res. Biogeosci. 115, 1012. https://doi.org/10.1029/2009JG001013.

Aitkenhead-Peterson, J.A., Steele, M.K., Nahar, N., Santhy, K., 2009. Dissolved organic carbon and nitrogen in urban and rural watersheds of south-Central Texas: land use and land management influences. Biogeochemistry 96, 119–129. https://doi.org/10.1007/S10533-009-9348-2/FIGURES/4.

Allen, R.G., Pereira, L.S., Raes, D., Smith, M., 1998. Crop Evapotranspiration - Guidelines for Computing Crop Water Requirements, FAO Irrigation and Drainage Paper 56. Rome.

ARPAV, 2021a. Fiumi - concentrazione dei parametri di base - Agenzia Regionale per la Prevenzione e Protezione Ambientale del Veneto [WWW document]. URL https://www.arpa.veneto.it/dati-ambientali/open-data/idrosfera/corsi-dacqua/fiumi-concentrazione-dei-parametri-di-base. (Accessed 8 January 2023).

ARPAV, 2021b. Bacini Idrografici del Piano di Tutela delle Acque - GeoPortale ARPAV [WWW document]. URL https://geomap.arpa.veneto.it/layers/geonode:bacinipta. (Accessed 4 March 2022) (accessed 1.8.23).

ARPAV, 2021c. Meteo e Clima, from 1994 to 2021 [WWW document]. URL https://www.arpa.veneto.it/dati-ambientali/open-data/clima. (Accessed 8 January 2023).

ARPAV, 2022. La rete idrometrica e le portate - Agenzia Regionale per la Prevenzione e Protezione Ambientale del Veneto [WWW Document]. URL https://www.arpa.veneto.it/temi-ambientali/idrologia/file-e-allegati/rapporti-e-documenti/idrologia-regionale/idrologia-regionale-la-rete-idrometrica. (Accessed 8 January 2023).

Aufdenkampe, A.K., Mayorga, E., Raymond, P.A., Melack, J.M., Doney, S.C., Alin, S.R., Aalto, R.E., Yoo, K., 2011. Riverine coupling of biogeochemical cycles between land, oceans, and atmosphere. Front. Ecol. Environ. 9, 53–60. https://doi.org/10.1890/100014.

Bastias, E., Bolivar, M., Ribot, M., Peipoch, M., Thomas, S.A., Sabater, F., Martí, E., 2020. Spatial heterogeneity in water velocity drives leaf litter dynamics in streams. Freshw. Biol. 65, 435–445. https://doi.org/10.1111/FWB.13436.

Battin, T.J., Kaplan, L.A., Findlay, S., Hopkinson, C.S., Marti, E., Packman, A.I., Newbold, J.D., Sabater, F., 2008. Biophysical controls on organic carbon fluxes in fluvial networks. Nat. Geosci. 1, 95–100. https://doi.org/10.1038/ngeo101.

Berggren, M., Al-Kharusi, E.S., 2020. Decreasing organic carbon bioreactivity in european rivers. Freshw. Biol. 65, 1128–1138. https://doi.org/10.1111/FWB.13498.

Borken, W., Ahrens, B., Schulz, C., Zimmermann, L., 2011. Site-to-site variability and temporal trends of DOC concentrations and fluxes in temperate forest soils. Glob. Chang. Biol. 17, 2428–2443. https://doi.org/10.1111/J.1365-2486.2011.02390.X.

Botter, G., Basso, S., Porporato, A., Rodriguez-Iturbe, I., Rinaldo, A., 2010. Natural streamflow regime alterations: damming of the piave river basin (Italy). Water Resour. Res. 46, 6522. https://doi.org/10.1029/2009WR008523.

Bouchez, J., Galy, V., Hilton, R.G., Gaillardet, J.Ô., Moreira-Turcq, P., Pérez, M.A., France-Lanord, C., Maurice, L., 2014. Source, transport and fluxes of Amazon River particulate organic carbon: insights from river sediment depth-profiles. Geochim. Cosmochim. Acta 133, 280–298. https://doi.org/10.1016/J.GCA.2014.02.032.

Boyer, E.W., Hornberger, G.M., Bencala, K.E., McKnight, D., 1996. Overview of a simple model describing variation of dissolved organic carbon in an upland catchment. Ecol. Model. 86, 183–188. https://doi.org/10.1016/0304-3800(95)00049-6.

Cai, Y., Guo, L., Wang, X., Aiken, G., 2015. Abundance, stable isotopic composition, and export fluxes of DOC, POC, and DIC from the lower Mississippi River during 2006–2008. J. Geophys. Res. Biogeosci. 120, 2273–2288. https://doi.org/10.1002/2015JG003139.

Camino-Serrano, M., Graf Pannatier, E., Vicca, S., Luyssaert, S., Jonard, M., Ciais, P., Guenet, B., Gielen, B., Peñuelas, J., Sardans, J., Waldner, P., Etzold, S., Cecchini, G., Clarke, N., GaliÄ, Z., Gandois, L., Hansen, K., Johnson, J., Klinck, U., Lachmanová, Z., Lindroos, A.J., Meesenburg, H., Nieminen, T.M., Sanders, T.G.M., Sawicka, K., Seidling, W., Thimonier, A., Vanguelova, E., Verstraeten, A., Vesterdal, L., Janssens, I.A., 2016. Trends in soil solution dissolved organic carbon (DOC) concentrations across European forests. Biogeosciences 13, 5567–5585. https://doi.org/10.5194/BG-13-5567-2016.

Camino-Serrano, M., Guenet, B., Luyssaert, S., Ciais, P., Bastrikov, V., De Vos, B., Gielen, B., Gleixner, G., Jornet-Puig, A., Kaiser, K., Kothawala, D., Lauerwald, R., Peñuelas, J., Schrumpf, M., Vicca, S., Vuichard, N., Walmsley, D., Janssens, I.A., 2018. ORCHIDEE-SOM: modeling soil organic carbon (SOC) and dissolved organic carbon (DOC) dynamics along vertical soil profiles in Europe. Geosci. Model Dev. 11, 937–957. https://doi.org/10.5194/GMD-11-937-2018.

Cattani, I., Fragoulis, G., Boccelli, R., Capri, E., 2006. Copper bioavailability in the rhizosphere of maize (Zea mays L.) grown in two italian soils. Chemosphere 64, 1972–1979. https://doi.org/10.1016/J.CHEMOSPHERE.2006.01.007.

Chanudet, V., Filella, M., 2008. Size and composition of inorganic colloids in a peri-alpine, glacial flour-rich lake. Geochim. Cosmochim. Acta 72, 1466–1479. https://doi.org/10.1016/J.GCA.2008.01.002.

Chen, D., Deng, X., Jin, G., Samie, A., Li, Z., 2017. Land-use-change induced dynamics of carbon stocks of the terrestrial ecosystem in Pakistan. Phys. Chem. Earth, Parts A/B/C 101, 13–20. https://doi.org/10.1016/J.PCE.2017.01.018.

Ciais, P., Sabine, C., Bala, G., Bopp, L., Brovkin, V., Canadell, J., Chhabra, A., DeFries, R., Galloway, J., Heimann, M., Jones, C., Le Quéré, C., Myneni, R.B., Piao, S., Thornto, P., 2013. Carbon and other biogeochemical cycles. In: Heinze, C., Tans, P., Vesala, T. (Eds.), Climate Change 2013: The Physical Science Basis. Contribution of Working Group I to the Fifth Assessment Report of the Intergovernmental Panel on Climate Change. Cambridge University Press, Cambridge, United Kingdom and New York, NY, USA, pp. 465–570.

Ciglenečki, I., Vilibić, I., Dautović, J., Vojvodić, V., Ćosović, B., Zemunik, P., Dunić, N., Mihanović, H., 2020. Dissolved organic carbon and surface active substances in the northern Adriatic Sea: long-term trends, variability and drivers. Sci. Total Environ. 730, 139104. https://doi.org/10.1016/j.scitotenv.2020.139104.

Comiti, F., Da Canal, M., Surian, N., Mao, L., Picco, L., Lenzi, M.A., 2011. Channel adjustments and vegetation cover dynamics in a large gravel bed river over the last 200 years. Geomorphology 125, 147–159. https://doi.org/10.1016/J.GEOMORPH.2010.09.011.

Currie, W., Aber, J., 1997. Modeling leaching as a decomposition process in humid montane forests. Ecology 78, 1844–1860.

da Silva Cruz, J., Blanco, C.J.C., de Oliveira Júnior, J.F., 2022. Modeling of land use and land cover change dynamics for future projection of the Amazon number curve. Sci. Total Environ. 811, 152348. https://doi.org/10.1016/J.SCITOTENV.2021.152348.

Dawson, J.J.C., Billett, M.F., Hope, D., Palmer, S.M., Deacon, C.M., 2004. Sources and sinks of aquatic carbon in a peatland stream continuum. URLBiogeochem 70, 71–92. https://doi.org/10.1023/B:BIOG.0000049337.66150.F1.

Dezsi, Ş., Mîndrescu, M., Petrea, D., Rai, P.K., Hamann, A., Nistor, M.-M., 2018. High-resolution projections of evapotranspiration and water availability for Europe under climate change. Int. J. Climatol. 38, 3832–3841. https://doi.org/10.1002/joc.5537.

Di Grazia, F., Gumiero, B., Galgani, L., Troiani, E., Ferri, M., Loiselle, S.A., 2021. Ecosystem services evaluation of nature-based solutions with the help of citizen scientists. Sustain. 13, 10629. https://doi.org/10.3390/SU131910629/S1.

Du, X., Zhang, X., Mukundan, R., Hoang, L., Owens, E.M., 2019. Integrating terrestrial and aquatic processes toward watershed scale modeling of dissolved organic carbon fluxes. Environ. Pollut. 249, 125–135. https://doi.org/10.1016/J.ENVPOL.2019.03.014.

Du, X., Loiselle, D., Alessi, D.S., Faramarzi, M., 2020. Hydro-climate and biogeochemical processes control watershed organic carbon inflows: development of an in-stream organic carbon module coupled with a process-based hydrologic model. Sci. Total Environ. 718, 137281. https://doi.org/10.1016/J.SCITOTENV.2020.137281.

Du, X., Faramarzi, M., Qi, J., Lei, Q., Liu, H., 2023. Investigating hydrological transport pathways of dissolved organic carbon in cold region watershed based on a watershed biogeochemical model. Environ. Pollut. 324, 121390. https://doi.org/10.1016/J.ENVPOL.2023.121390.

EFAS, 2018. Assessment report on the flood events in Spain and Italy during autumn 2018 | Copernicus EMS - European Flood Awareness System [WWW Document]. URL https://www.efas.eu/en/report/assessment-report-flood-events-spain-and-italy-during-autumn-2018. (Accessed 25 October 2022).

Einarsdottir, K., Wallin, M.B., Sobek, S., 2017. High terrestrial carbon load via groundwater to a boreal lake dominated by surface water inflow. J. Geophys. Res. Biogeosci. 122, 15–29. https://doi.org/10.1002/2016JG003495.

Fröberg, M., Berggren Kleja, D., Hagedorn, F., 2007. The contribution of fresh litter to dissolved organic carbon leached from a coniferous forest floor. Eur. J. Soil Sci. 58, 108–114. https://doi.org/10.1111/J.1365-2389.2006.00812.X.

Futter, M.N., de Wit, H.A., 2008. Testing seasonal and long-term controls of streamwater DOC using empirical and process-based models. Sci. Total Environ. 407, 698–707. https://doi.org/10.1016/J.SCITOTENV.2008.10.002.

Futter, M.N., Butterfield, D., Cosby, B.J., Dillon, P.J., Wade, A.J., Whitehead, P.G., 2007. Modeling the mechanisms that control in-stream dissolved organic carbon dynamics in upland and forested catchments. Water Resour. Res. 43, 2424. https://doi.org/10.1029/2006WR004960.

Galgani, L., Tognazzi, A., Rossi, C., Ricci, M., Angel Galvez, J., Dattilo, A.M., Cozar, A., Bracchini, L., Loiselle, S.A., 2011. Assessing the optical changes in dissolved organic matter in humic lakes by spectral slope distributions. J. Photochem. Photobiol. B Biol. 102, 132–139. https://doi.org/10.1016/J.JPHOTOBIOL.2010.10.001.

Galy, V., Eglinton, T., France-Lanord, C., Sylva, S., 2011. The provenance of vegetation and environmental signatures encoded in vascular plant biomarkers carried by the Ganges-Brahmaputra rivers. Earth Planet. Sci. Lett. 304, 1–12. https://doi.org/10.1016/J.EPSL.2011.02.003.

Gommet, C., Lauerwald, R., Ciais, P., Guenet, B., Zhang, H., Regnier, P., 2022. Spatiotemporal patterns and drivers of terrestrial dissolved organic carbon (DOC) leaching into the european river network. Earth Syst. Dyn. 13, 393–418. https://doi.org/10.5194/ESD-13-393-2022.

Guswa, A.J., Hamel, P., Meyer, K., 2017. Curve number approach to estimate monthly and annual direct runoff. J. Hydrol. Eng. 23, 04017060. https://doi.org/10.1061/(ASCE)HE.1943-5584.0001606.

Hamel, P., Valencia, J., Schmitt, R., Shrestha, M., Piman, T., Sharp, R.P., Francesconi, W., Guswa, A.J., 2020. Modeling seasonal water yield for landscape management: applications in Peru and Myanmar. J. Environ. Manag. 270, 110792. https://doi.org/10.1016/J.JENVMAN.2020.110792.

Harrison, J.A., Caraco, N., Seitzinger, S.P., 2005. Global patterns and sources of dissolved organic matter export to the coastal zone: results from a spatially explicit, global model. Glob. Biogeochem. Cycles 19. https://doi.org/10.1029/2005GB002480.

Iravani, M., White, S.R., Farr, D.R., Habib, T.J., Kariyeva, J., Faramarzi, M., 2019. Assessing the provision of carbon-related ecosystem services across a range of temperate grassland systems in western Canada. Sci. Total Environ. 680, 151–168. https://doi.org/10.1016/J.SCITOTENV.2019.05.083.

ISPRA, 2018. Corine Land Cover 2018 IV livello | Uso, copertura e consumo di suolo [WWW document]. URL https://groupware.sinanet.isprambiente.it/uso-copertura-e-consumo-di-suolo/library/copertura-del-suolo/corine-land-cover/corine-land-cover-2018-iv-livello. (Accessed 8 January 2023).

ISPRA, 2020. Istituto Superiore per la Protezione e la Ricerca Ambientale, SINANet. DEM 20 m Italy [WWW document]. URL http://www.sinanet.isprambiente.it/it/sia-ispra/download-mais/dem20/view. (Accessed 8 January 2023).

Jutras, M.F., Nasr, M., Castonguay, M., Pit, C., Pomeroy, J.H., Smith, T.P., Zhang, C.Fu, Ritchie, C.D., Meng, F.R., Clair, T.A., Arp, P.A., 2011. Dissolved organic carbon concentrations and fluxes in forest catchments and streams: DOC-3 model. Ecol. Model. 222, 2291–2313. https://doi.org/10.1016/J.ECOLMODEL.2011.03.035.

Kalbitz, K., Schmerwitz, J., Schwesig, D., Matzner, E., 2003. Biodegradation of soil-derived dissolved organic matter as related to its properties. Geoderma 113, 273–291. https://doi.org/10.1016/S0016-7061(02)00365-8.

Kalev, S., Toor, G.S., 2020. Concentrations and loads of dissolved and particulate organic carbon in urban stormwater runoff. Water 12, 1031. https://doi.org/10.3390/W12041031 2020, Vol. 12, Page 1031.

Kim, J.K., Jung, S., Jang, C., Lee, Y., Owen, J.S., Jung, M.S., Kim, B., Sung, Eom J., 2013. Dissolved and Particulate Organic Carbon Concentrations in Stream Water and Relationships With Land Use in Multiple-use Watersheds of the Han River (Korea). 38, pp. 326–339. https://doi.org/10.1080/02508060.2013.769411.

Krinner, G., Viovy, N., de Noblet-Ducoudré, N., Ogée, J., Polcher, J., Friedlingstein, P., Ciais, P., Sitch, S., Prentice, I.C., 2005. A dynamic global vegetation model for studies of the coupled atmosphere-biosphere system. Glob. Biogeochem. Cycles 19, 1–33. https://doi.org/10.1029/2003GB002199.

Lessels, J.S., Tetzlaff, D., Carey, S.K., Smith, P., Soulsby, C., 2015. A coupled hydrology–biogeochemistry model to simulate dissolved organic carbon exports from a permafrost-influenced catchment. Hydrol. Process. 29, 5383–5396. https://doi.org/10.1002/HYP.10566.

Li, M., Peng, C., Wang, M., Xue, W., Zhang, K., Wang, K., Shi, G., Zhu, Q., 2017. The carbon flux of global rivers: a re-evaluation of amount and spatial patterns. Ecol. Indic. 80, 40–51. https://doi.org/10.1016/J.ECOLIND.2017.04.049.

Lindström, G., Johansson, B., Persson, M., Gardelin, M., Bergström, S., 1997. Development and test of the distributed HBV-96 hydrological model. J. Hydrol. 201, 272–288. https://doi.org/10.1016/S0022-1694(97)00041-3.

Loiselle, S.A., Bracchini, L., Cózar, A., Dattilo, A.M., Tognazzi, A., Rossi, C., 2009. Variability in photobleaching yields and their related impacts on optical conditions in subtropical lakes. J. Photochem. Photobiol. B Biol. 95, 129–137. https://doi.org/10.1016/J.JPHOTOBIOL.2009.02.002.

Luo, X., Bai, X., Tan, Q., Ran, C., Chen, H., Xi, H., Chen, F., Wu, L., Li, C., Zhang, S., Zhong, X., Tian, S., 2022. Particulate organic carbon exports from the terrestrial biosphere controlled by erosion. Catena 209, 105815. https://doi.org/10.1016/J.CATENA.2021.105815.

Maniquiz, M.C., Lee, S., Kim, L.H., 2010. Multiple linear regression models of urban runoff pollutant load and event mean concentration considering rainfall variables. J. Environ. Sci. 22, 946–952. https://doi.org/10.1016/S1001-0742(09)60203-5.

Melillo, J.M., McGuire, A.D., Kicklighter, D.W., Moore, B., Vorosmarty, C.J., Schloss, A.L., 1993. Global climate change and terrestrial net primary production. Nature 3636426 (363), 234–240. https://doi.org/10.1038/363234a0.

Melton, J.R., Arora, V.K., Wisernig-Cojoc, E., Seiler, C., Fortier, M., Chan, E., Teckentrup, L., 2020. CLASSIC v1.0: the open-source community successor to the Canadian land surface scheme (CLASS) and the Canadian terrestrial ecosystem model (CTEM)-part 1: model framework and site-level performance. Geosci. Model Dev. 13, 2825–2850. https://doi.org/10.5194/GMD-13-2825-2020.

Michalzik, B., Tipping, E., Mulder, J., Gallardo Lancho, J.F., Matzner, E., Bryant, C.L., Clarke, N., Lofts, S., Vicente Esteban, M.A., 2003. Modelling the production and transport of dissolved organic carbon in forest soils. Biogeochemistry 66, 241–264. https://doi.org/10.1023/B:BIOG.0000005329.68861.27/METRICS.

Nakhavali, M., Lauerwald, R., Regnier, P., Guenet, B., Chadburn, S., Friedlingstein, P., 2021. Leaching of dissolved organic carbon from mineral soils plays a significant role in the terrestrial carbon balance. Glob. Chang. Biol. 27, 1083–1096. https://doi.org/10.1111/GCB.15460.

Neff, J.C., Asner, G.P., 2001. Dissolved organic carbon in terrestrial ecosystems: synthesis and a model. Ecosystems 4, 29–48. https://doi.org/10.1007/S100210000058/METRICS.

Némery, J., Mano, V., Coynel, A., Etcheber, H., Moatar, F., Meybeck, M., Belleudy, P., Poirel, A., 2013. Carbon and suspended sediment transport in an impounded alpine river (Isère, France). Hydrol. Process. 27, 2498–2508. https://doi.org/10.1002/HYP.9387.

Nistor, M.M., Man, T.C., Benzaghta, M.A., Nedumpallile Vasu, N., Dezsi, Ş., Kizza, R., 2018. Land cover and temperature implications for the seasonal evapotranspiration in europe. Geogr. Tech. 13, 85–108. https://doi.org/10.21163/GT_2018.131.09.

NRCS-USDA, 2007. NRCS engineering manuals and handbooks | Natural Resources Conservation Service [WWW Document]. URL https://www.nrcs.usda.gov/conservation-basics/conservation-by-state/north-dakota/nrcs-engineering-manuals-and-handbooks. (Accessed 8 January 2023).

Ortiz-Hernández, J., Lucho-Constantino, C., Lizárraga-Mendiola, L., Beltrán-Hernández, R.I., Coronel-Olivares, C., Vázquez-Rodríguez, G., 2016. Quality of urban runoff in wet and dry seasons: a case study in a semi-arid zone. Environ. Sci. Pollut. Res. 23, 25156–25168. https://doi.org/10.1007/S11356-016-7547-7/FIGURES/3.

Parton, W.J., Scurlock, J.M.O., Ojima, D.S., Gilmanov, T.G., Scholes, R.J., Schimel, D.S., Kirchner, T., Menaut, J.-C., Seastedt, T., Garcia Moya, E., Kamnalrut, A., Kinyamario, J.I., 1993. Observations and modeling of biomass and soil organic matter dynamics for the grassland biome worldwide. Glob. Biogeochem. Cycles 7, 785–809. https://doi.org/10.1029/93GB02042.

Perdue, E.M., Reuter, J.H., Ghosal, M., 1980. The operational nature of acidic functional group analyses and its impact on mathematical descriptions of acid-base equilibria in humic substances. Geochim. Cosmochim. Acta 44, 1841–1851. https://doi.org/10.1016/0016-7037(80)90233-1.

Pettine, M., Patrolecco, L., Camusso, M., Crescenzio, S., 1998. Transport of carbon and nitrogen to the northern Adriatic Sea by the Po River. Estuar. Coast. Shelf Sci. 46, 127–142. https://doi.org/10.1006/ecss.1997.0303.

QGIS Development Team, 2022. QGIS geographic information system. Open source geospatial foundation project. QGIS v.3.22. Geographic information system API documentation. QGIS Association. [WWW document]. URL https://qgis.org/en/site/. (Accessed 8 January 2023).

Qi, J., Du, X., Zhang, X., Lee, S., Wu, Y., Deng, J., Moglen, G.E., Sadeghi, A.M., McCarty, G.W., 2020. Modeling riverine dissolved and particulate organic carbon fluxes from two small watersheds in the northeastern United States. Environ. Model. Softw. 124, 104601. https://doi.org/10.1016/J.ENVSOFT.2019.104601.

Qu, H.J., Kroeze, C., 2010. Past and future trends in nutrients export by rivers to the coastal waters of China. Sci. Total Environ. 408, 2075–2086. https://doi.org/10.1016/J.SCITOTENV.2009.12.015.

Raymond, P.A., Saiers, J.E., Sobczak, W.V., 2016. Hydrological and biogeochemical controls on watershed dissolved organic matter transport: pulse-shunt concept. Ecology 97, 5–16. https://doi.org/10.1890/14-1684.1.

Roulet, N., Moore, T.R., 2006. Browning the waters. Nature 4447117 (444), 283–284. https://doi.org/10.1038/444283a.

Samson, C.C., Rajagopalan, B., Summers, R.S., 2016. Modeling source water TOC using hydroclimate variables and local polynomial regression. Environ. Sci. Technol. 50, 4413–4421. https://doi.org/10.1021/ACS.EST.6B00639/SUPPL_FILE/ES6B00639_SI_001.PDF.

Sharp, R., Tallis, H.T., Ricketts, T., Guerry, A.D., Wood, S.A., Chaplin-Kramer, R., Nelson, E., Wolny, S., Olwero, N., Vigerstol, K., Pennington, D., Mendoza, G., Aukema, J., Foster, J., Forrest, J., Cameron, D., Arkema, K., Lonsdorf, E., Kennedy, C., Verutes, G., Kim, C.K., Guannel, G., Papenfus, M., Toft, J., Marsik, M., Bernhardt, J., Griffin, R., Glowinski, K., Chaumont, N., Perelman, A., Lacayo, M., Mandle, L., Hamel, P., Vogl, A.L., Rogers, L., Bierbower, W., Denu, D., Douglass, J., D, E., 2018. InVEST 3.6.0 user's guide [WWW document]. URLNat. Cap. Proj. http://data.naturalcapitalandresilienceplatform.org/invest-releases/documentation/current_release/index.html.

Siudek, P., Frankowski, M., Siepak, J., 2015. Seasonal variations of dissolved organic carbon in precipitation over urban and forest sites in Central Poland. Environ. Sci. Pollut. Res. 22, 11087–11096. https://doi.org/10.1007/S11356-015-4356-3/FIGURES/5.

Smith, J., Gottschalk, P., Bellarby, J., Chapman, S., Lilly, A., Towers, W., Bell, J., Coleman, K., Nayak, D., Richards, M., Hillier, J., Flynn, H., Wattenbach, M., Aitkenhead, M., Yeluripati, J., Farmer, J., Milne, R., Thomson, A., Evans, C., Whitmore, A., Falloon, P., Smith, P., 2010. Estimating changes in Scottish soil carbon stocks using ECOSSE. I. Model description and uncertainties. Clim. Res. 45, 179–192. https://doi.org/10.3354/CR00899.

Spencer, R.G.M., Hernes, P.J., Ruf, R., Baker, A., Dyda, R.Y., Stubbins, A., Six, J., 2010. Temporal controls on dissolved organic matter and lignin biogeochemistry in a pristine tropical river, Democratic Republic of Congo. J. Geophys. Res. Biogeosci. 115, 3013. https://doi.org/10.1029/2009JG001180.

Steinberg, C.E.W., 2003. Ecology of humic substances in freshwaters. Ecology of Humic Substances in Freshwaters, 1st ed Springer Berlin Heidelberg, Berlin, Heidelberg https://doi.org/10.1007/978-3-662-06815-1.

Strohmeier, S., Knorr, K.H., Reichert, M., Frei, S., Fleckenstein, J.H., Peiffer, S., Matzner, E., 2013. Concentrations and fluxes of dissolved organic carbon in runoff from a forested catchment: insights from high frequency measurements. Biogeosciences 10, 905–916. https://doi.org/10.5194/BG-10-905-2013.

Surian, N., Rinaldi, M., Pellegrini, L., Audisio, C., Maraga, F., Teruggi, L., Turitto, O., Ziliani, L., 2009. Channel adjustments in northern and Central Italy over the last 200 years. Spec. Pap. Geol. Soc. Am. 451, 83–95. https://doi.org/10.1130/2009.2451(05).

Tague, C.L., Band, L.E., 2004. RHESSys: regional hydro-ecologic simulation system—an object-oriented approach to spatially distributed modeling of carbon, water, and nutrient cycling. Earth Interact. 8, 1–42. https://doi.org/10.1175/1087-3562(2004)8<1:rrhsso>2.0.co;2.

Thurman, E.M., 1985. Organic geochemistry of natural waters. Organic Geochemistry of Natural Waters, 1st ed Springer Netherlands https://doi.org/10.1007/978-94-009-5095-5.

Tian, H., Yang, Q., Najjar, R.G., Ren, W., Friedrichs, M.A.M., Hopkinson, C.S., Pan, S., 2015. Anthropogenic and climatic influences on carbon fluxes from eastern North America to the Atlantic Ocean: a process-based modeling study. J. Geophys. Res. Biogeosci. 120, 757–772. https://doi.org/10.1002/2014JG002760.

van den Berg, L.J.L., Shotbolt, L., Ashmore, M.R., 2012. Dissolved organic carbon (DOC) concentrations in UK soils and the influence of soil, vegetation type and seasonality. Sci. Total Environ. 427–428, 269–276. https://doi.org/10.1016/J.SCITOTENV.2012.03.069.

Von Wachenfeldt, E., Tranvik, L.J., 2008. Sedimentation in boreal lakes - the role of flocculation of allochthonous dissolved organic matter in the water column. Ecosystems 11, 803–814. https://doi.org/10.1007/S10021-008-9162-Z/FIGURES/5.

Wheatcroft, R.A., Goñi, M.A., Hatten, J.A., Pasternack, G.B., Warrick, J.A., 2010. The role of effective discharge in the ocean delivery of particulate organic carbon by small, mountainous river systems. Limnol. Oceanogr. 55, 161–171. https://doi.org/10.4319/LO.2010.55.1.0161.

Worrall, F., Burt, T., 2005. Predicting the future DOC flux from upland peat catchments. J. Hydrol. 300, 126–139. https://doi.org/10.1016/J.JHYDROL.2004.06.007.

Wu, H., Peng, C., Moore, T.R., Hua, D., Li, C., Zhu, Q., Peichl, M., Arain, M.A., Guo, Z., 2014. Modeling dissolved organic carbon in temperate forest soils: TRIPLEX-DOC model development and validation. Geosci. Model Dev. 7, 867–881. https://doi.org/10.5194/gmd-7-867-2014.

Xu, Z., Fan, W., Wei, H., Zhang, P., Ren, J., Gao, Z., Ulgiati, S., Kong, W., Dong, X., 2019. Evaluation and simulation of the impact of land use change on ecosystem services based on a carbon flow model: a case study of the Manas River Basin of Xinjiang, China. Sci. Total Environ. 652, 117–133. https://doi.org/10.1016/J.SCITOTENV.2018.10.206.

Yang, Q., Zhang, X., 2016. Improving SWAT for simulating water and carbon fluxes of forest ecosystems. Sci. Total Environ. 569–570, 1478–1488. https://doi.org/10.1016/J.SCITOTENV.2016.06.238.

Zhang, X., Izaurralde, R.C., Arnold, J.G., Williams, J.R., Srinivasan, R., 2013. Modifying the soil and water assessment tool to simulate cropland carbon flux: model development and initial evaluation. Sci. Total Environ. 463–464, 810–822. https://doi.org/10.1016/J.SCITOTENV.2013.06.056.

Zhang, H., Lauerwald, R., Ciais, P., Van Oost, K., Guenet, B., Regnier, P., 2022. Global changes alter the amount and composition of land carbon deliveries to European rivers and seas. URLCommun. Earth Environ. 3, 1–11. https://doi.org/10.1038/s43247-022-00575-7.

Zomer, R.J., Trabucco, A., 2022. Global Aridity Index and Potential Evapo-Transpiration (ET 0) Database v3, pp. 1–6.